Conventional quantum phase transition driven by complex parameter in non-Hermitian $\mathcal{PT}$-symmetric Ising model

C. Li, G. Zhang, X. Z. Zhang and Z. Song*
School of Physics, Nankai University, Tianjin 300071, China

A conventional quantum phase transition (QPT) can be accessed by varying a real parameter at absolute zero temperature. Motivated by the discovery of the pseudo-Hermiticity of non-Hermitian systems, we explore the QPT in non-Hermitian $\mathcal{PT}$-symmetric Ising model, which is driven by a staggered complex transverse field. Exact solution shows that the Laplacian of the groundstate energy density, with respect to real and imaginary components of the transverse field, diverges on the boundary in the complex plane. The phase diagram indicate that the imaginary transverse field has the effect of shrinking the paramagnet phase. In addition, we also investigate the connection between the geometric phase and the QPT.

PACS numbers: 11.30.Er, 64.70.Tg, 03.65.Vf

arXiv:1404.0805v1 [quant-ph] 3 Apr 2014

I. INTRODUCTION

Quantum phase transitions (QPTs) happen at zero temperature when physical parameters are changed, inducing dramatic changes in the ground-state properties [1]. So far, these system-specific parameters are required to be real, which can be a magnetic field in spin systems [2, 3], the intensity of a laser beam in cold-atom simulators of Hubbard-like models [4], the dopant concentration in high-Tc superconductors [5], etc.

With the discovery that a non-Hermitian Hamiltonian having simultaneous parity-time ($\mathcal{PT}$) symmetry has a real spectrum [6], there has been an intense effort to establish a $\mathcal{PT}$-symmetric quantum theory as a complex extension of the conventional quantum mechanics [7–14]. Motivated by the pseudo-Hermiticity of non-hermitian systems, it is natural to ask whether a complex parameter can drive a QPT. Here the QPT does not include the phase transition in the context of the complex quantum mechanics, which happens when the reality of the spectrum does not ensure diagonalizability, associating with spontaneous $\mathcal{PT}$-symmetry breaking. As system parameter varying, a sudden changes in the eigenstate rather than specifying the ground state and the critical point is referred as exceptional point.

In traditional condensed matter approaches, for the case of second-order QPTs, the critical point is identified by the divergence of the second-order derivative of the ground state density, with respect to the real parameter. It is interesting to investigate the QPT of a non-Hermitian system, where the transition is driven by the competition between real and imaginary parts of parameter.

In this paper, we explore the QPT in non-Hermitian $\mathcal{PT}$-symmetric Ising model, which is driven by a staggered complex transverse field. Exact solution shows that the Laplacian of the groundstate energy density, with respect to real and imaginary components of the transverse field, diverges on the boundary in the complex plane. The phase diagram indicates that the imaginary transverse field has the effect of shrinking the paramagnet phase. We also investigate the connection between the geometric phase and the QPT in the present model as that in the study of the conventional quantum spin model. We find that the phase boundary can be identified by divergence of Berry curvature density.

This paper is organized as follows. In Section II, we present the model Hamiltonian, where the Ising ring is subjected to a staggered complex magnetic field. The exact solution allows us to identify the role of the complex field. In Section III, we investigate the phase diagram by the Laplacian of the groundstate energy density. Section IV is devoted to another characterization of the QPT in terms of the geometric phase of the ground state. Finally, we give a summary and discussion in Section V.

II. MODEL AND SOLUTION

We consider a non-Hermitian one-dimensional spin-1/2 Ising model in a complex staggered transverse magnetic field on a $2N$-site lattice. The system is modeled by the following Hamiltonian

$$\mathcal{H} = -J\sum_{j=1}^{2N}\left(\sigma_j^z\sigma_{j+1}^z + g_j\sigma_j^x\right), \tag{1}$$

where $g_j = \eta + (-1)^{j+1/2}\,\xi$ with η and ξ being real numbers. Here σ_j^λ ($\lambda = x, z$) are the Pauli operators on site j, and satisfy the periodic boundary condition $\sigma_j^\lambda \equiv \sigma_{j+2N}^\lambda$. We note that the non-Hermiticity of the Hamiltonian arises from complex staggered transverse magnetic field. One can define a parity operator $\mathcal{P}$ which has the function

$$\mathcal{P}\sigma_j^\lambda\mathcal{P}^{-1} \equiv \sigma_{2N+1-j}^\lambda, \tag{2}$$

and a time reversal operator $\mathcal{T}$ which has the function

$$\mathcal{T}\sigma_j^\lambda\mathcal{T}^{-1} \equiv \begin{cases} -\sigma_j^\lambda, \lambda = y \\ \sigma_j^\lambda, \lambda = x, z \end{cases}, \tag{3}$$

* songtc@nankai.edu.cn

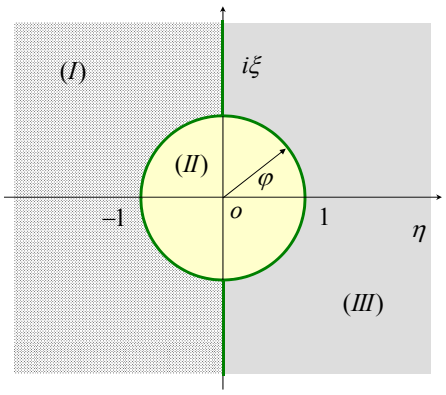

FIG. 1. (Color online) Phase diagram for the ground state of the Ising ring in a a staggered complex transverse field. The heavy lines represent the boundary which separates three quantum phases. Phases I and III are paramagnet, while II is ferromagnet.

It turns out that, for nonzero ξ, we have $[\mathcal{P},\mathcal{H}]\neq 0$ and $[\mathcal{T},\mathcal{H}]\neq 0$, but

$$[\mathcal{PT},\mathcal{H}]=0, \tag{4}$$

where the antilinear time reversal operator $\mathcal{T}$ has the function $\mathcal{T}i\mathcal{T}=-i$, i.e., the Hamiltonian $\mathcal{H}$ is parity-time ($\mathcal{PT}$) reversal invariant.

Now we consider the solution of the non-Hermitian Hamiltonian of Eq. (1). We start by taking the Jordan-Wigner transformation [15]

$$\sigma_j^+ = \prod_{l<j}\left(1-2c_l^\dagger c_l\right)c_j, \tag{5}$$

$$\sigma_j^- = \prod_{l<j}\left(1-2c_l^\dagger c_l\right)c_j^\dagger, \tag{6}$$

$$\sigma_j^x = 1-2c_j^\dagger c_j, \tag{7}$$

$$\sigma_j^z = -\prod_{l<j}\left(1-2c_l^\dagger c_l\right)\left(c_j+c_j^\dagger\right), \tag{8}$$

to replace the Pauli operators by the fermionic operators c_j. Likewise, the parity of the number of fermions

$$\Pi=\prod_{l=1}^{2N}(\sigma_l^x)=(-1)^{N_p} \tag{9}$$

is a conservative quantity, i.e., $[\mathcal{H},\Pi]=0$, where $N_p=\sum_{j=1}^{2N}c_j^\dagger c_j$. Then the Hamiltonian (1) can be rewritten as

$$\mathcal{H}=\sum_{\zeta=+,-}P_\zeta\mathcal{H}_\zeta P_\zeta, \tag{10}$$

where

$$P_\zeta=\frac{1}{2}\left(1+\zeta\Pi\right) \tag{11}$$

is the projector on the subspaces with even ($\zeta=+$) and odd ($\zeta=-$) N_p. The Hamiltonian in each invariant subspaces has the form

$$\begin{aligned}\mathcal{H}_\zeta=&-J\sum_{j=1}^{2N-1}\left(c_j^\dagger c_{j+1}+c_{j+1}^\dagger c_j+c_j^\dagger c_{j+1}^\dagger+c_{j+1}c_j\right)\\&+J\zeta\left(c_{2N}^\dagger c_1+c_1^\dagger c_{2N}+c_{2N}^\dagger c_1^\dagger+c_1c_{2N}\right)\\&-Jg_j\sum_{j=1}^{2N-1}\left(1-2c_j^\dagger c_j\right)\end{aligned} \tag{12}$$

taking the Fourier transformation

$$c_j=\frac{1}{\sqrt{N}}\sum_{k_\zeta}e^{ik_\zeta j}\begin{cases}\alpha_{k_\zeta}, & \text{even } j\\ \beta_{k_\zeta}, & \text{odd } j\end{cases}, \tag{13}$$

for the Hamiltonians $\mathcal{H}_\zeta$, we have

$$\mathcal{H}_\zeta=-J\sum_{k_\zeta}H_{k_\zeta} \tag{14}$$

$$\begin{aligned}H_{k_\zeta}=&\left(e^{ik}+1\right)\alpha_{k_\zeta}^\dagger\beta_{k_\zeta}+\left(e^{ik}-1\right)\alpha_{k_\zeta}^\dagger\beta_{-k_\zeta}^\dagger+\text{H.c.}\\&+2\eta-2\left(\eta+i\xi\right)\alpha_{k_\zeta}^\dagger\alpha_{k_\zeta} \qquad (15)\\&-2\left(\eta-i\xi\right)\beta_{k_\zeta}^\dagger\beta_{k_\zeta} \qquad (16)\end{aligned}$$

where the momentum k_ζ are defined as $k_+=2\left(m+1/2\right)\pi/N$, $k_-=2m\pi/N$, $m=0,1,2,...,N-1$, respectively.

In the following, we focus on the subspace with $\zeta=+$ since it turns out that the ground state lies in this sector in the thermodynamic limit. We will neglect the subscript ζ in $\mathcal{H}_\zeta$ and k_ζ. In order to diagonalize the Hamiltonian $\mathcal{H}$, we introduce the composite operators $\overline{\Lambda}_n^k$ ($n\in[1,6]$), defined as

$$\begin{aligned}\overline{\Lambda}_n^k=&\frac{1}{\Omega_n^k}[e^{ik/2}\alpha_k^\dagger\beta_{-k}^\dagger-e^{-ik/2}\beta_k^\dagger\alpha_{-k}^\dagger\\&+2\cos\left(k/2\right)\left(\frac{\alpha_k^\dagger\alpha_{-k}^\dagger}{\epsilon_n^k+i2\xi}+\frac{\beta_k^\dagger\beta_{-k}^\dagger}{\epsilon_n^k-i2\xi}\right)\\&-2i\sin\left(k/2\right)\left(\frac{1}{\epsilon_n^k+2\eta}\alpha_k^\dagger\beta_k^\dagger\alpha_{-k}^\dagger\beta_{-k}^\dagger+\frac{1}{\epsilon_n^k-2\eta}\right)],\\&\left(n\in[1,5]\right),\end{aligned} \tag{17}$$

where the normalization factor is

$$\begin{aligned}\left(\Omega_n^k\right)^2=&2+\frac{4\cos^2\left(k/2\right)}{\left(\epsilon_n^k+2i\xi\right)^2}+\frac{4\cos^2\left(k/2\right)}{\left(\epsilon_n^k-2i\xi\right)^2}\\&+\frac{4\sin^2\left(k/2\right)}{\left(\epsilon_n^k+2\eta\right)^2}+\frac{4\sin^2\left(k/2\right)}{\left(\epsilon_n^k-2\eta\right)^2},\end{aligned} \tag{18}$$

and

$$\overline{\Lambda}_6^k=\frac{1}{\sqrt{2}}\left(e^{ik/2}\alpha_k^\dagger\beta_{-k}^\dagger+e^{-ik/2}\beta_k^\dagger\alpha_{-k}^\dagger\right). \tag{19}$$

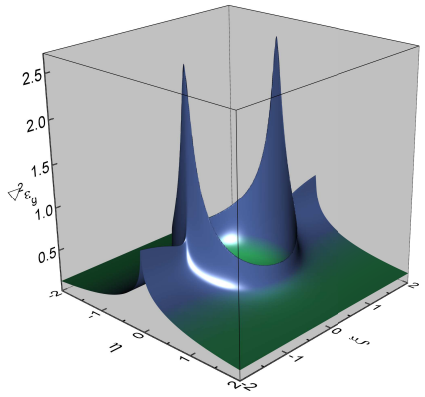

FIG. 2. (Color online) The Laplacian of the groundstate energy density ε_g as a function of the field for the case $N = 300$. The peaks mark the clear regions of criticality.

Here coefficients ϵ_n^k are defined as

$$\begin{aligned}\epsilon_1^k &= \sqrt{2r^2\cos(2\varphi) + 2\sqrt{r^4 - 2r^2\cos k + 1} + 2},\\ \epsilon_3^k &= \sqrt{2r^2\cos(2\varphi) - 2\sqrt{r^4 - 2r^2\cos k + 1} + 2},\\ \epsilon_2^k &= -\epsilon_1^k,\ \epsilon_4^k = -\epsilon_3^k,\ \epsilon_5^k = \epsilon_6^k = 0,\end{aligned} \tag{20}$$

where we parameterize the complex field in terms of the polar radius and angle

$$r = \sqrt{\eta^2 + \xi^2} \text{ and } \tan\varphi = \xi/\eta, \tag{21}$$

as shown in figure 1. Similarly, we also introduce the composite operators Λ_n^k by the following procedure

$$\Lambda_n^k = \left[\overline{\Lambda}_n^k(\xi \to -\xi)\right]^\dagger, \tag{22}$$

which will be used to construct the biorthogonal set together with $\overline{\Lambda}_n^k$. Straightforward calculation shows that

$$\langle 0|\Lambda_m^{k'}\overline{\Lambda}_n^k|0\rangle = \delta_{mn}\delta_{kk'}, \tag{23}$$

and

$$h_k\overline{\Lambda}_n^k|0\rangle = 2\epsilon_n^k\overline{\Lambda}_n^k|0\rangle, \tag{24}$$

$$\langle 0|\Lambda_m^k h_k^\dagger = \langle 0|\Lambda_m^k 2\epsilon_n^k, \tag{25}$$

where $h_k = H_k + H_{-k}$ and $|0\rangle$ is the vaccum of fermion operator c_j, i.e., $c_j|0\rangle = 0$. Eq. (23) indicates the biorthogonality relation between the eigenstates of H_k. Accordingly, all the eigenstates of $\mathcal{H}$ can be constructed by the product of complete biorthogonal basis set $\left\{\overline{\Lambda}_n^k|0\rangle\right\}$ as the form $\prod_{\{k,n\}}\overline{\Lambda}_n^k|0\rangle$. It can be seen that part of eigenvalues of $\mathcal{H}$ can be complex, which does not affect our investigation.

In the following analysis, we will focus on the ground state (or the eigen state with the lowest real eigenvalue) of the Hamiltonian. The ground state of $\mathcal{H}$ can be constructed as the form

$$|G\rangle = \prod_{0<k<\pi}\overline{\Lambda}_1^k|0\rangle, \tag{26}$$

with the eigenvalue

$$E_g = -2\sum_k \epsilon_1^k. \tag{27}$$

where $k = 2\pi(m + 1/2)/N$, $m = 0, 1, 2, \ldots, N/2 - 1$. Accordingly the bra ground state can be expressed as the form

$$\langle\overline{G}| = \langle 0|\prod_{0<k<\pi}\Lambda_1^k. \tag{28}$$

It is worth stressing that the diagonalization procedure we have used here is a little different from the Bogoliubov transformation which is applied for the standard transverse-field Ising model [16]. Here Λ_n^k and $\overline{\Lambda}_n^k$ are composite operators, which do not obey the canonical commutation relations as the fermion operators in the Bogoliubov transformation, but the biorthonormal relation in Eq. (23).

III. PHASE DIAGRAM

In this section, we will investigate the phase diagram of the Hamiltonian (1) based on the solutions. In all previous study for a non-Hermitian system, the term phase diagram has a little different meaning from that of a Hermitian system. It usually represents the region in which the non-Hermitian Hamiltonian has full real spectrum or not (as examples of non-Hermitian quantum spin systems, see Ref. [17, 18]), rather than the quantum phase transition in a Hermitian system[1], which specifies the sudden change of the ground state as a real parameter varies. However, in this paper, we are interested in the sudden change of the state $|G\rangle$ as the complex field g_j varies. The aim of this work is to investigate the conventional QPT occurs in the present non-Hermitian spin system.

To this aim, we investigate the value of ϵ_1^k at $k = 0$, which is

$$\epsilon_1^0 = \sqrt{2r^2\cos(2\varphi) + 2|r^2 - 1| + 2}. \tag{29}$$

We note that ϵ_1^0 has a discontinuous derivative at $r = 1$. On the other hand, for $r > 1$, we have

$$\epsilon_1^0 = 2r|\cos\varphi|, \tag{30}$$

which indicates a discontinuous derivative at $\eta = 0$. These boundary lines separate the ground state into three phases as illustrated in Fig. 1, with I and III being paramagnet, II being ferromagnet. Quantum phase transition takes place at the critical value $r = 1$ and $\eta = 0$

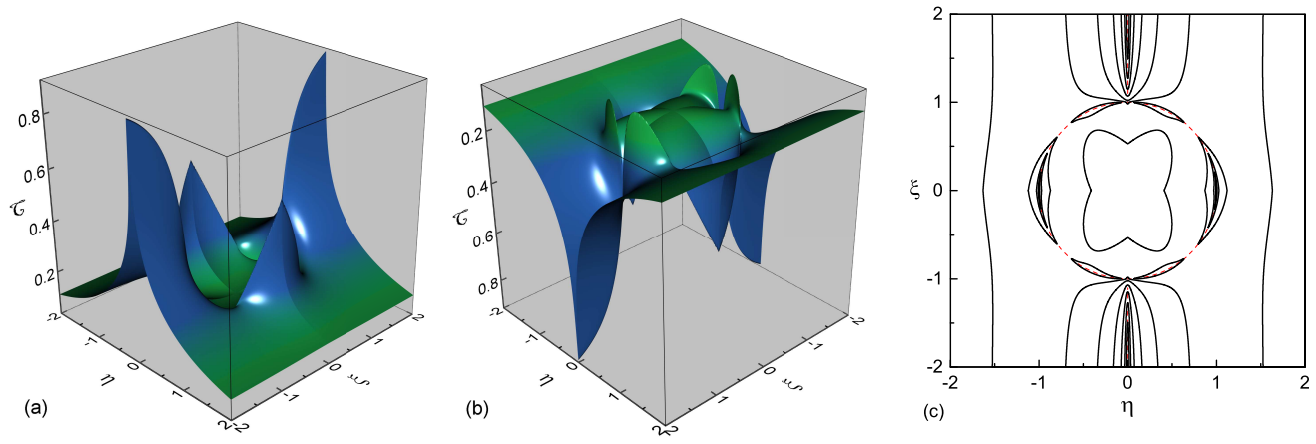

FIG. 3. (Color online) (a) The curvature density $\mathcal{C}$ as a function of the field for the Hamiltonians with the parameters of (a) Eq. (52), and $N = 300$. The plots (b) is the inversion of (a). The dips and peaks indicate the quasi-critical lines. (c) Contour map of $\mathcal{C}$. The red dashed lines indicate the phase diagram in Fig. 1.

$(r > 1)$ of external field. When $\eta \gg 1$ $(-\eta \gg 1)$, then the ground state is a paramagnet $\prod_{l=1}^{2N} |\rightarrow\rangle_l$ $(\prod_{l=1}^{2N} |\leftarrow\rangle_l)$ with all spins polarized up (down) along the x axis. In this limit case, the imaginary field ξ has no contribution to the groundstate energy. On the other hand, when $r = 0$, then there are two degenerate ferromagnetic ground states with all spins pointing either up or down along the z axis: $\prod_{l=1}^{2N} |\uparrow\rangle_l$ or $\prod_{l=1}^{2N} |\downarrow\rangle_l$. It can be seen that nonzero imaginary field ξ seems to suppress the influence of the Ising term $\sum \sigma_j^z \sigma_{j+1}^z$, shrinking the ferromagnetic phase area in the η axis.

Now we further investigate the behavior of groundstate energy density $\varepsilon_g = E_g/(2N)$ as function of η and ξ in the following two cases: i) for $\eta \neq 0$ when r crosses 1, ii) $|\xi| \gg 1$, when η crosses 0. To characterize this situation, we calculate the Laplacian of ε_g

$$\nabla^2 \varepsilon_g = \frac{\partial^2 \varepsilon_g}{\partial \xi^2} + \frac{\partial^2 \varepsilon_g}{\partial \eta^2}, \tag{31}$$

which will reduce to second derivative of the groundstate energy density of the standard transverse-field Ising model [1] with respect to the transverse field η when we take $\xi = 0$. The physical meaning of $\nabla^2 \varepsilon_g$ will be given in the next section.

i) The case of $\eta \neq 0$ and $r \to 1$. The main contribution of the Laplacian of ε_g near this boundary can be expressed as

$$\nabla^2 \varepsilon_g \sim \sum_k \frac{2\sqrt{2} r \sin^2 k}{N \epsilon_1^k \left(r^4 - 2r^2 \cos k + 1\right)^{3/2}} \tag{32}$$

In the thermodynamic limit we have

$$\nabla^2 \varepsilon_g \approx \int_0^\pi F(k)\, \mathrm{d}k, \tag{33}$$

where the integrand is defined as

$$F(k) = \frac{\sqrt{2} r \sin^2 k}{\pi \epsilon_1^k \left(r^4 - 2r^2 \cos k + 1\right)^{3/2}}. \tag{34}$$

We are interested in the divergent behavior when $r^2 \sim 1$. We note that the main contribution comes from $k \in [0, \delta]$ with $\delta \ll \pi$. Then we have

$$\nabla^2 \varepsilon_g \approx \int_0^\delta F(k)\, \mathrm{d}k \approx -\frac{\sqrt{2}}{\pi |\cos \varphi|} \ln |r - 1|. \tag{35}$$

ii) The case of $|\xi| \gg 1$ and $\eta \to 0$. By the similar analysis as above, we have

$$\nabla^2 \varepsilon_g \approx \frac{\sqrt{2}}{\pi} \int_0^\delta \frac{1}{\epsilon_1^k} dk \approx -\frac{\sqrt{2}}{\pi} \ln |\eta|. \tag{36}$$

Then we conclude that the Laplacian of ε_g is divergent at the boundary illustrated in Fig. 1.

It is crucial to stress that such phase separation does not arise from the breaking of the symmetries defined by Eqs. (4) as that in non-Hermitian systems have been investigated heretofore. It is easy to check that

$$\mathcal{PT} |G\rangle = \pm |G\rangle \tag{37}$$

which indicates that the ground state have $\mathcal{PT}$ symmetries in all region, due to the relations

$$\mathcal{PT} \alpha_k^\dagger \left(\beta_k^\dagger\right) (\mathcal{PT})^{-1} = -e^{-2ik} \beta_k^\dagger \alpha_k^\dagger \tag{38}$$

$$\mathcal{PT} \left(\overline{\Lambda}_1^k\right) (\mathcal{PT})^{-1} = -\overline{\Lambda}_1^k \tag{39}$$

We conclude this section by presenting the numerical simulation of $\nabla^2 \varepsilon_g$ as function of the complex field for finite N system. In Fig. 2 we plot the Laplacian of ε_g for the case $N = 300$. We observe that the regions of criticality are clearly marked by a sudden increase of the value of $\nabla^2 \varepsilon_g$. As before in the Hermitian system, we ascribe this type of behavior to a dramatic change in the structure of the ground state of the system while undergoing QPT.

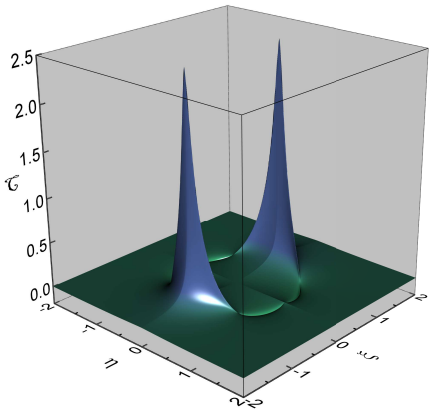

FIG. 4. (Color online) The curvature density $\mathcal{C}$ as a function of the field for the Hamiltonians with the parameters of Eq. (56), and $N = 300$. The peaks only indicate the quasi-critical lines of the circle in the Fig. 1, but not the straight lines on the ξ axis.

IV. BERRY CURVATURE

In the present section, we study the geometric phase for the ground state in the vicinity of the quantum phase boundary. In the realm of traditional quantum mechanics, geometric phase has been introduced to analyze the quantum phase transitions of the XY model [19–21], and much effort has been devoted to various Hermitian many-body systems [22–30]. A natural question is whether or not the geometric phase of the ground state in the present model can be utilized to characterize the quantum phase boundary. With particular form of parameter dependence on the external field, we will show that the boundary corresponds to the divergence of the Berry curvature.

We consider a family of the Hamiltonians that can be obtained by applying a rotation of θ_a and θ_b around the x-direction for spins in sublattice A and B, respectively. We have

$$H(\theta_a, \theta_b) = R(\theta_a, \theta_b) H R^{\dagger}(\theta_a, \theta_b) \tag{40}$$

with the unitary operator

$$R(\theta_a, \theta_b) = \prod_{l_a, l_b} e^{i\sigma^x_{l_a}\theta_a} e^{i\sigma^x_{l_b}\theta_b}. \tag{41}$$

The family of Hamiltonians that is parameterized by real θ_a, θ_b is clearly isospectral and, therefore, the critical behavior is independent from θ_a, θ_b. In addition, due to its bilinear form, $H(\theta_a, \theta_b)$ is π-periodic in θ_a, θ_b. The Hamiltonian $H(\theta_a, \theta_b)$ can be diagonalized by a standard procedure. And the corresponding ground state is

$$|g(\theta_a, \theta_b)\rangle = R(\theta_a, \theta_b) |G\rangle , \tag{42}$$

and the bra ground state is

$$\langle \overline{g}(\theta_a, \theta_b)| = \langle \overline{G}| R^{\dagger}(\theta_a, \theta_b), \tag{43}$$

where θ_a and θ_b are assumed to be the functions of the complex field, $\theta_{a,b} = \theta_{a,b}(\eta, \xi)$. In the following, we will demonstrate that a appropriate choice of $\theta_{a,b}(\eta, \xi)$ can connect the geometric phase of the ground state to the boundary of the phase diagram.

The Berry curvature for the ground state is an anti-symmetric second-rank tensor derived from the Berry connection via

$$\mathcal{G}_{\xi\eta} = \frac{\partial}{\partial \xi}\mathcal{B}_{\eta} - \frac{\partial}{\partial \eta}\mathcal{B}_{\xi}, \tag{44}$$

where

$$\mathcal{B}_{\lambda} = i \sum_{\nu=a,b} \frac{\partial \theta_{\nu}}{\partial \lambda} \langle \overline{G}| \sum_{l_{\nu}} \sigma^x_{l_{\nu}} |G\rangle \tag{45}$$

$$+ \langle \overline{G}| \partial_{\lambda} G\rangle , \quad (\lambda = \eta, \xi) . \tag{46}$$

where we set

$$|\partial_{\lambda} G\rangle \equiv \frac{\partial}{\partial \lambda} |G\rangle , \ \langle \partial_{\lambda} \overline{G}| \equiv \frac{\partial}{\partial \lambda} \langle \overline{G}|$$

Straightforward derivation shows that

$$\langle \partial_{\xi} \overline{G}| \partial_{\eta} G\rangle - \langle \partial_{\eta} \overline{G}| \partial_{\xi} G\rangle = 0, \tag{47}$$

which indicates that in the case of $\partial\theta_{\nu}/\partial\lambda = 0$, the Berry curvature vanishes. In that case, the adiabatic evolution along a loop in the $\eta - \xi$ plane is trivial, cannot generate a nonzero geometric phase. This is what happens for the original Hamiltonian in Eq. (1), yielding nothing on the boundary of the phase diagram from the aspect of geometric phase of the ground state.

As a consequence of the field-dependent phase factor $\theta_{a,b}$, we have the curvature density $\mathcal{C} = \mathcal{G}_{\xi\eta}/(2N)$,

$$\mathcal{C} = \frac{i}{2} \sum_{\nu=a,b} \left(\frac{\partial \theta_{\nu}}{\partial \eta} \frac{\partial}{\partial \xi} - \frac{\partial \theta_{\nu}}{\partial \xi} \frac{\partial}{\partial \eta} \right) m_{\nu}, \tag{48}$$

where

$$m_{\nu} = \frac{1}{N} \langle \overline{G}| \sum_{l_{\nu}} \sigma^x_{l_{\nu}} |G\rangle , \tag{49}$$

is defined as the magnetization of sublattice $\nu = a, b$ for the ground state $|G\rangle$. On the other hand, from the Hellmann–Feynman theorem, it is easy to obtain

$$m_a = (m_b)^* = \frac{1}{N} \langle \overline{G}| \frac{\partial H}{\partial (\eta - i\xi)} |G\rangle \tag{50}$$

$$= \frac{2\partial \varepsilon_g}{\partial \eta} + i \frac{2\partial \varepsilon_g}{\partial \xi}.$$

It is now possible to investigate the physical meaning of the Laplacian of ε_g. From the definition of m_a, it is immediate to check that

$$\nabla^2 \varepsilon_g = \frac{1}{4} \left[\frac{\partial (m_a + m_b)}{\partial \eta} - i \frac{\partial (m_a - m_b)}{\partial \xi} \right], \tag{51}$$

which displays the connection between $\nabla^2\varepsilon_g$ and the magnetizations.

We now proceed to examine the critical behavior of Berry curvature density $\mathcal{G}_{\xi\eta}/(2N)$. Unlike $\nabla^2\varepsilon_g$, the result depends on the functions of $\theta_{a,b}$. If the phase factors are taken in the simple form

$$\theta_a = \theta_b = \eta + \xi, \tag{52}$$

the Berry curvature density is explicitly given by

$$\mathcal{C} = i2\left(\frac{\partial^2\varepsilon_g}{\partial\xi\partial\eta} - \frac{\partial^2\varepsilon_g}{\partial\eta^2}\right). \tag{53}$$

For this quantity we follow the same steps as in last section. i) The case of $\eta \neq 0$ and $r^2 \sim 1$: In the thermodynamic limit, the main contribution of $\mathcal{G}_{\xi\eta}/2N$ near this boundary can be expressed as

$$\mathcal{C} \backsim \chi(\varphi)\int_0^\pi F(k)\,dk \approx -\frac{\sqrt{2}\chi(\varphi)}{\pi|\cos\varphi|}\ln|r-1|, \tag{54}$$

where $\chi(\varphi) = \left[\sin(2\varphi) - 2\cos^2\varphi\right]$. We can see the prefactor $\chi(\varphi)/|\cos\varphi|$ vanishes at $\varphi = \pi/4,\ 5\pi/4$, and is discontinuous at $\varphi = \pi/2,\ 3\pi/2$. It indicates that the curvature density C is not divergent at the two vanishing points.

ii) The case of $|\xi| \gg 1$ and $|\eta| \to 0$. By the similar analysis as above, we have

$$\mathcal{C} \approx -\frac{4\sqrt{2}}{\pi}\int_0^\delta \frac{1}{\epsilon_1^k}\mathrm{d}k \approx -\frac{4\sqrt{2}}{\pi}\ln|\eta|. \tag{55}$$

We note that the Berry curvature density is divergent at the boundary of the phase diagram, as what happens in a Hermitian system. However, the Berry curvature is not an imaginary number as that in a Hermitian system. This is due to the fact that the evolution is non-unitary for a non-Hermitian system. Nevertheless, the biorthogonal norm is still conserved under the evolution. It is worth pointing out that the choice of the function in Eq. (52) is crucial for the occurrence of the divergence of the Berry curvature density. For instance, if we take

$$\theta_a = -\theta_b = \eta + \xi, \tag{56}$$

the Berry curvature density has the form $\mathcal{C} = 2\left(\partial^2\varepsilon_g/\partial\xi\partial\eta - \partial^2\varepsilon_g/\partial\xi^2\right)$, which is divergent on the boundary $r = 1$ but not at $\eta = 0$.

We perform the numerical simulation of the curvature densities $\mathcal{C}$ for the Hamiltonians with the parameters of Eqs. (52) and (56). The shapes of $\mathcal{C}$ accord with the analytical predictions in both cases.

V. SUMMARY

In this paper, we explore the QPT in non-Hermitian $\mathcal{PT}$-symmetric Ising model, which is driven by a staggered complex transverse field. Exact solution shows that the Laplacian of the groundstate energy density, with respect to real and imaginary components of the transverse field, diverges on the boundary in the complex plane. The phase diagram indicates that the imaginary transverse field has the effect of shrinking the paramagnet phase. We also investigate the connection between the geometric phase and the QPT in the present model as that in the study of the conventional quantum spin model. We find that the phase boundary can be identified by divergence of Berry curvature density.

ACKNOWLEDGMENTS

We acknowledge the support of the National Basic Research Program (973 Program) of China under Grant No. 2012CB921900 and CNSF (Grant No. 11374163).

[1] S. Sachdev, *Quantum Phase Transition* (Cambridge University Press, Cambridge, 1999).
[2] R. Coldea, D. A. Tennant, E. M. Wheeler, E. Wawrzynska, D. Prabhakaran, M. Telling, K. Habicht, P. Smeibidl, and K. Kiefer, Science 327, 177 (2010).
[3] L. E. Sadler, J. M. Higbie, S. R. Leslie, M. Vengalattore and D. M. Stamper-Kurn, Nature (London) 443, 312 (2006).
[4] M. Greiner, O. Mandel, T. Esslinger, T. W. Hänsch, and I. Bloch, Nature (London) 415, 39 (2002); R. Jördens, N. Strohmaier, K. Günter, H. Moritz, and T. Esslinger, Nature (London) 455, 204 (2008); M. Lewenstein, A. Sanpera, V. Ahufinger, B. Damski, A. Sen(De), and U. Sen, Adv. Phys. 56, 243 (2007).
[5] P. A. Lee, N. Nagaosa, and X.-G. Wen, Rev. Mod. Phys. 78, 17 (2006).
[6] C. M. Bender, and S. Boettcher, Phys. Rev. Lett. **80**, 5243 (1998).
[7] C. M. Bender, S. Boettcher, and P. N. Meisinger, J. Math. Phys. **40**, 2201 (1999).
[8] P. Dorey, C. Dunning, and R. Tateo, J. Phys. A: Math. Gen. **34**, L391 (2001); P. Dorey, C. Dunning, and R. Tateo, J. Phys. A: Math. Gen. **34**, 5679 (2001).
[9] C. M. Bender, D. C. Brody, and H. F. Jones, Phys. Rev. Lett. **89**, 270401 (2002).
[10] A. Mostafazadeh, J. Math. Phys. **43**, 3944 (2002).
[11] A. Mostafazadeh and A. Batal, J. Phys. A: Math. Gen. **37**, 11645 (2004).
[12] A. Mostafazadeh, J. Phys. A: Math. Gen. **36**, 7081 (2003).
[13] H. F. Jones, J. Phys. A: Math. Gen. **38**, 1741 (2005).
[14] A. Mostafazadeh, J. Math. Phys. **43**, 2814 (2002).
[15] P. Jordan and E. Wigner, Z. Physik **47**, 631 (1928).

[16] E. Lieb, T. Schulz and D. Mattis, Ann. Phys. (NY) 16, 407 (1961).
[17] X. Z. Zhang and Z. Song, Phys. Rev. A **87**, 012114 (2013).
[18] X. Z. Zhang and Z. Song, Phys. Rev. A **87**, 042108 (2013).
[19] A. C. M. Carollo and J. K. Pachos, Phys. Rev. Lett. **95**, 157203 (2005).
[20] S. L. Zhu, Phys. Rev. Lett. **96**, 077206 (2006).
[21] S. L. Zhu, Int. J. Mod. Phys. B **22**, 561 (2008).
[22] G. Chen, J. Q. Li, and J. Q. Liang, Phys. Rev. A **74**, 054101 (2006).
[23] X. X. Yi and W. Wang, Phys. Rev. A **75**, 032103 (2007).
[24] L. C. Venuti and P. Zanardi, Phys. Rev. Lett. **99**, 095701 (2007).
[25] Y. Q. Ma and S. Chen, Phys. Rev. A **79**, 022116 (2009); Y. Q. Ma, S. Chen, H. Fan, and W. M. Liu, Phys. Rev. B **81**, 245129 (2010).
[26] T. Liu, Y. Y. Zhang, Q. H. Chen, and K. L. Wang, Phys. Rev. A **80**, 023810 (2009).
[27] X. Z. Yuan, H. S. Goan, and K. D. Zhu, Phys. Rev. A **81**, 034102 (2010).
[28] X. M. Lu and X. G. Wang, Europhys. Lett. **91**, 30003 (2010).
[29] S. C. Li, L. B. Fu, and J. Liu, Phys. Rev. A **84**, 053610 (2011); L. D. Zhang and L. B. Fu, Europhys. Lett. **93**, 30001 (2011); S. C. Li and L. B. Fu, Phys. Rev. A **84**, 023605 (2011).
[30] Z. G. Yuan, P. Zhang, S. S. Li, J. Jing, and L. B. Kong, Phys. Rev. A **85**, 044102 (2012).